Biogeochemistry (2010) 99:15–30
DOI 10.1007/s10533-009-9394-9

SYNTHESIS AND EMERGING IDEAS

Patterns of hydrologic control over stream water total nitrogen to total phosphorus ratios

Mark B. Green · Jacques C. Finlay

Received: 20 November 2008 / Accepted: 12 November 2009 / Published online: 9 December 2009

Abstract Many ecologists and biogeochemists explore the interaction of the nitrogen (N) and phosphorus (P) cycles by addressing N:P ratios. While N:P ratios are recognized as broadly important to the composition and functioning of lotic ecosystems, the fundamental controls on stream water N:P ratio variation remains poorly understood. Low N:P ratio (less than 16) streams appear more likely in arid climates than in mesic climates, suggesting possible hydrologic or landscape controls. We explored the importance of watershed hydrology to the variation of total N to total P (TN:TP) ratios in stream water, and whether such variation is characteristically different across watershed classes based on mean annual precipitation and median observed TN:TP ratio. Nonparametric scatter plot analysis was applied to normalized TN:TP ratios and associated discharge (Q) measurements from 57 minimally-impacted watersheds from the contiguous United States. At the seasonal scale, TN:TP ratios showed a negative relationship with Q in semiarid climates and a positive relationship with Q in humid climates. Over storm event scales, TN:TP ratios decline with increasing Q across all watershed classes. The results broadly indicate hydrology is an important driver of TN:TP ratio variation over multiple time scales. We hypothesize that the broad differences across watershed classes are driven by variation in the nature of connectivity (frequency and magnitude of connections) of the landscape to streams. A strong physical control of N:P ratios in stream water is in stark contrast to the biological control of N:P ratios in the oceans, suggesting that application of stoichiometric theory—developed using marine systems—to lotic systems requires a broader consideration of controlling factors.

Keywords Catchment hydrology · Connectivity · N:P ratios · Stoichiometry · Stream ecology

M. B. Green (✉)
Graduate Program of Water Resources Science, University of Minnesota, St. Paul, MN, USA
e-mail: mbgreen@plymouth.edu

M. B. Green · J. C. Finlay
National Center for Earth Surface Dynamics, Minneapolis, MN, USA

Present Address:
M. B. Green
Center for the Environment, Plymouth State University, Plymouth, NH, USA

M. B. Green
Northern Research Station, U.S. Forest Service, Durham, NH, USA

J. C. Finlay
Department of Ecology, Evolution, and Behavior, University of Minnesota, Minneapolis, MN, USA

Introduction

Redfield (1958) demonstrated the large-scale, integrated stoichiometric nitrogen (N) and phosphorus (P) requirements of marine phytoplankton by showing the similar inorganic N:P ratio in water and seston in Earth's oceans. He concluded that the similar N:P ratios were due to the specific cellular demands of phytoplankton and their subsequent decomposition. Marine systems represent an end-member on the spectrum of aquatic ecosystem water residence time; lotic systems represent the opposite side of the residence time spectrum (UNEP 2002; Green et al. 2009). Therefore, the shorter residence time in lotic ecosystems should cause less of a signature from in situ biotic activity in water chemistry and more of a watershed signature (vegetation, soils, and aquatic ecosystem processes). As evidence, algal stoichiometry is infrequently reflected in stream water nutrient stoichiometry (Francoeur et al. 1999; Stelzer and Lamberti 2001; Green and Fritsen 2006). While Redfield's seston decomposition mechanism explains large-scale variation of marine water N:P ratios, a mechanism explaining large-scale variation of stream water N:P ratios remains elusive.

Many studies have examined the role of nutrient sources on aquatic ecosystem N:P ratios. Downing and McCauley (1992) explored the role of different nutrient sources in driving the variability of N:P ratios in lakes. They summarized the N:P ratio of many nutrient sources and suggested that human disturbance is the primary driver of N:P ratio variability, causing lower lake water N:P ratios. Billen et al. (1991) similarly focused on nutrient sources, especially from human disturbances, as driving the variability of N:P ratios of river loads to Earths oceans. Turner et al. (2003) emphasized the role of human disturbance and increase of N inputs to global rivers causing higher dissolved inorganic N:P ratios in disturbed rivers. Others have focused on N and P sources from agriculture as altering freshwater N:P ratios (Arbuckle and Downing 2001; Ptacnik et al. 2005). Bedrock geology and soil types have also been suggested to influence nutrient stoichiometry in streams (Borchardt 1996; McGroddy et al. 2008). While the role of nutrient sources, especially driven by human disturbance, is an important component to N:P ratio variability, hydrologic transport also plays an important role.

Watershed transport pathways are a driver of N:P ratio variability. Horne and Goldman (1994) suggest that the increased erosion in arid watersheds is what causes their tendency of lower N:P ratios. Watson et al. (1981) showed how the N:P ratio of nutrient loads decreased as urbanization and associated overland runoff increased. Correll et al. (1999) demonstrated the role of storms in driving the temporal variability of N:P ratios, with the lowest N:P ratios occurring during the largest storms. Detenbeck et al. (2004) showed a positive correlation between watershed storage (wetlands and lakes) and N:P ratios. The role of watershed flow paths has received recent attention, demonstrating high N:P ratios of subsurface water compared to surface water (Saunders et al. 2006). Green et al. (2007) showed how watershed flow paths caused different N:P ratios during storm events in two adjacent basins. Hydrologic connectivity has been demonstrated as an important factor to stream water nutrient stoichiometry in monitored (Frost et al. 2009) and simulated watersheds (Green and Wang 2008). The studies addressing watershed flow paths have all been conducted at relatively small spatial scales which makes the fundamental role of flow pathways in controlling N:P ratios hard to elucidate.

Stream water N:P stoichiometry in minimally-impacted watersheds apparently varies with mean annual precipitation (Grimm et al. 1981; McGroddy et al. 2008), providing a large-scale pattern that may aid the pursuit of a fundamental mechanism behind stream water N:P ratio variation. To better understand this pattern, we present a synthesis relating TN:TP ratios to stream discharge (Q) across two temporal scales (seasonal and event) in a set of minimally-impacted watersheds from the United States. We hypothesize that watershed hydrology, represented by Q, is an underlying driver of the variation of stream water N:P ratios, and can help explain the spatial and temporal patterns of stream water N:P ratios.

Methods

Nutrient and discharge data

This study used total nitrogen (TN) and total phosphorus (TP) samples and discharge (Q) rates collected by the United States Geological Survey (USGS;

http://waterdata.usgs.gov/nwis) from 57 minimally-impacted watersheds across the contiguous United States (Table 1). The watersheds were sampled generally at monthly or bi-weekly intervals between 1970 and 2007. Although these watersheds have been used to estimate background nutrient concentrations in rivers (Smith et al. 2003), they do include some level of human disturbance, ranging from elevated atmospheric deposition of N in the northeast to regional agriculture influence on ground water N concentrations in the midwest. We focused on the total fractions of N and P because they include the entire bioavailable pool (Dodds 2003) and the non-bioavailable fraction may become bioavailable during longitudinal transport (Pacini and Gachter 1999).Total P samples ($n = 7459$) included 31% of the samples with concentrations that were below analytical detection, in which case the detection limit was used as the concentration value. The TN analysis included 4358 samples. Analysis of the TN data is presented in Green and Finlay (2008), with this study adding a comparison of TN dynamics across watersheds of different median TN:TP ratios, as described below. The TN:TP ratios were calculated as a molar ratio, and only samples with detected TN or TP were included in this analysis (one could be below detection), which resulted in 3970 TN:TP data points. The Q measurement associated with each TN or TP sample was extracted from the USGS database. Some relevant analysis of Q is presented in Green and Finlay (2008).

Data analysis

The watershed data were analyzed using the Nonparametric Smoothing of Normalized Variables (NSNV) and Nonparametric Thinning of Normalized Variables (NTNV) techniques described in Green and Finlay (2008). As a brief summary, both the NSNV and NTNV techniques use data which have been normalized by a "local" reference percentile; "local" indicating that data from a specific gage are normalized by a percentile determined from all data at the same gage. The normalization method for a variable, V, follows:

$$V^* = \log_{10}\left(\frac{V_w}{V_{w,P_V}}\right) \quad (1)$$

where V^* is the normalized variable (e.g., nutrient concentration), V_w is an observation at gage w, and V_{w,P_V} is the reference observation at gage w corresponding to percentile P_V. By the definition of V^*, data values greater than the reference value, V_{w,P_V}, will have a normalized value greater than 0. Conversely, data values less than V_{w,P_V} will have a normalized value less than 0.

The NSNV method evaluates the seasonal variability of normalized variables. The method smoothes seasonal V^* data, plotted versus day of the year, by calculating a weight ratio within a defined smoothing window. The window width must be defined; 59 days produced suitably smooth curves and was thus used for our analysis (Green and Finlay 2008). The smoothing window passes across the data from a window center of 1 to 365 in one-day increments. Within the smoothing window the weight ratio of the data indicates the relative weight of all data in the window. Formally, the weight ratio is defined as the sum of the V^* with values greater than 0 divided by the absolute value of the sum of the V^* with values less than 0. If the weight ratio is less than 1, the data in the window have greater weight below the P_V than above the P_V, and a weight ratio greater than 1 indicates that the data in the window have greater weight above the P_V than below the P_V. As an example, a weight ratio of 10 indicates that the data weight above the P_V is 10 times greater than below the P_V. For the NSNV analysis, all of the TN, TP, and TN:TP data points were normalized by the local median concentration or ratio ($P_V = 50$).

Seasonal variability of TN:TP, as indicated by the NSNV analysis, was compared directly to Q by plotting the TN:TP* weight ratio curve versus the Q^* weight ratio curve. The resulting curves show the generalized seasonal relationship between TN:TP ratio and Q, and also indicate any hysteresis. Hysteresis of solute concentrations across the rising and falling limbs of a hydrograph indicates the number of different water pathways and the timing of each pathways contribution to stream flow (Evans and Davies 1998; House and Warwick 1998) or could indicate temporal chemical evolution of one water source. Evans and Davies (1998) presented a series of hypothetical hysteresis curves that would result from the different solute sources that are transported during different stages of the storm hydrograph. Applications of the concentration versus discharge hysteresis models dominantly focus on the storm event timescale; we apply the models at the seasonal timescale.

Table 1 Gage identification information, mean annual precipitation (P_m), and median TN:TP ratio from the sites used in this study

USGS gage ID	Name	P_m (mm)	Median TN:TP (mol:mol)
1054200	Wild River, ME	1113	66
1137500	Ammonoosuc River, NH	1134	69
1170100	Green River, CT	1270	81
1362200	Ecopus Creek, NY	1041	76
1434025	Biscuit Brook, NY	1095	104
1466500	McDonalds Branch, NJ	1080	54
1545600	Young Womans Creek, PA	1057	105
2038850	Holiday Creek, VA	1080	44
2084557	Van Swamp, NC	1355	117
2135300	Scape Ore Swamp, SC	1101	81
2229000	Middle St. Marys River, FL	1397	96
2327100	Sopchoppy River, FL	1468	59
2337500	Snake Creek, GA	1397	29
2369800	Blackwater River, AL	1651	111
2450250	Sipsey Fork, AL	1410	66
2479155	Cypress Creek, MS	1651	82
3237280	Upper Twin Creek, OH	1078	91
3460000	Catalooche Creek, NC	1420	49
4001000	Washington Creek, MI	763	100
4063700	Popple River, WI	808	70
5124480	Kawishiwi River, MN	701	88
6169500	Rock Creek, MT	318	32
6623800	Encampment Creek, WY	518	61
6719505	Clear Creek, CO	559	34
6752000	Cache la Poudre River, CO	483	55
6753400	Lonetree Creek, CO	404	100
6775900	Dismal River, NE	516	9
6879650	Kings Creek, KS	826	49
6929315	Paddy Creek, MO	1080	58
7056000	Buffalo River, AR	1085	46
7060710	North Sylamore Creek, AR	1097	62
7083000	Halfmoon Creek, CO	459	73
7340300	Cossatot River, AR	1390	55
7373000	Big Creek, LA	1397	33
8103900	South Fork Rocky Creek, TX	769	66
8227000	Saguache Creek, CO	399	6
8313350	Rito de los Frijoles, NM	350	17
8377900	Rio Mora, NM	392	66
9352900	Vallecito Creek, CO	514	75
9430600	Mogollon Creek, NM	515	44
9508300	Wet Bottom Creek, AZ	516	55
10172200	Red Butte Creek, UT	523	18
10244950	Steptoe Creek, NV	330	67
10249300	South Twin Creek, NV	327	55

Table 1 continued

USGS gage ID	Name	P_m (mm)	Median TN:TP (mol:mol)
10309000	East Fork Carson, NV	684	17
10343500	Sagehen Creek, CA	621	37
10346000	Truckee River, CA	621	30
11264500	Merced River, CA	952	55
11475560	Elder Creek, CA	1732	33
12416000	Hayden Creek, ID	690	67
12447390	Andrews Creek, WA	854	53
13010065	Snake River, WY	1055	33
13018300	Cache Creek, WY	767	44
13120500	Big Lost River, ID	516	35
13169500	Big Jacks Creek, ID	356	26
13331500	Minam River, OR	885	44
14200400	Little Abiqua Creek, OR	1550	65
14203750	Gales Creek, OR	1381	37

The NTNV method produces a curve that shows concentration variation due to Q variation. The following steps produce the NTNV curves. Q values at each gage are converted to percentiles in order to collapse the variability between gages onto a common scale. The dependent variable (TN concentration, TP concentration, or TN:TP ratio) was normalized by the local median at a gage in order to collapse the variability between gages. The normalized concentration weight ratios are evaluated from 1st to 99th percentile Q (P_Q). At each P_Q, the data with Q greater than the P_Q are isolated and the $\text{Quad}_{\text{I:IV}}$ weight ratio—the ratio of the sum of Manhattan distances from (P_Q, 1) above and below the median concentration—is calculated. The Q data below the P_Q are also isolated and the $\text{Quad}_{\text{II:III}}$ weight ratio is calculated. Calculation of the $\text{Quad}_{\text{I:IV}}$ and $\text{Quad}_{\text{II:III}}$ weight ratio from $P_Q = 1$ to $P_Q = 99$ results in the NTNV curves. Further details about the method are outlined in Green and Finlay (2008).

The NSNV and NTNV methods rcapture dynamics occurring at different time scales. The NSNV curves show periodic variation and damp out stochastic variation, while the NTNV curves include information from seasonal and stochastic variation (Sabo and Post 2008). Variation in discharge percentile is driven by seasonality (as shown in the NSNV method) and storm events (hours to days). By organizing the data using only Q, and not temporal information (i.e., day of year), the NTNV curves are much more informative about the variation of a concentration or concentration ratio due only to Q. Concentration variation in NSNV curves are partially driven by Q, but also include other seasonally evolving processes—like changes in nutrient cycling in terrestrial ecosystems (e.g. variable nitrate production and retention in soils). Thus, the plots of TN:TP* weight ratios versus Q* weight ratios primarily indicate seasonal periodic variability.

Uncertainty around the NSNV and NTNV curves was estimated using nonparametric bootstrap resampling, described in Green and Finlay (2008). We report the 95% confidence interval as the uncertainty.

Subsets of the global TN, TP, and TN:TP data were defined by mean annual precipitation in a watershed and median TN:TP ratios at a gage. The mean annual precipitation subsets were defined as semiarid (precipitation <600 mm; 18 watersheds), subhumid ($1200 \geq$ precipitation ≤ 600; 25 watersheds; $n = 1798$), and humid (precipitation > 1200; 14 watersheds). The TN:TP ratio subsets were defined as low (TN:TP ≤ 35; 13 watersheds), intermediate ($65 \geq$ TN:TP > 35; 21 watersheds), and high (TN:TP > 65; 23 watersheds). The relationship between median observed TN:TP ratio and mean annual precipitation, and thus the overlap of the two catchment classifications, is shown in Fig. 1. Each mean annual precipitation and median TN:TP ratio

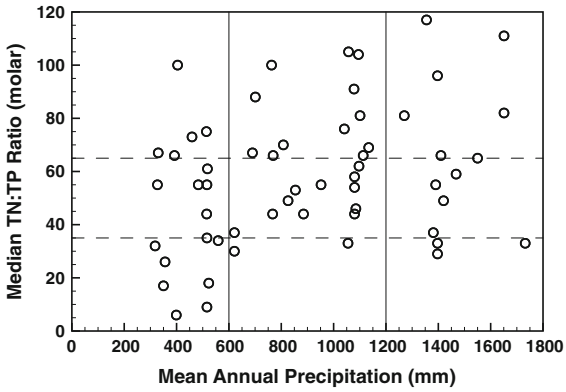

Fig. 1 Median observed TN:TP ratio versus mean annual precipitation from the sites used in this study. The *vertical solid lines* separate the semiarid, subhumid, and humid climate subgroups and the *horizontal dashed lines* separate the low, intermediate, and high median TN:TP ratio subgroups

subset was analyzed separately with NSNV and NTNV.

Both the mean annual precipitation and median TN:TP ratio subsets had a notable geographical structure. For the precipitation subsets, the semiarid watershed subset consisted of primarily mountainous headwater streams from the western United States where early season snow melt is a substantial feature of the annual hydrograph (see Green and Finlay 2008). The humid watersheds were primarily from the southeastern and northwestern United States, where snow is a much smaller influence on stream flow, and temperatures and terrestrial dynamics show less seasonal variation than in the colder climates. It should be noted that use of just one variable—mean annual precipitation—to separate watersheds put two distinct regions like the southeast and northwest United States into the same group. While geology, geomorphology, land cover, and atmospheric deposition are distinctly different between these regions, our purpose was to test for an overall signal of mean annual precipitation as a primary driver of N:P stoichiometry. For the TN:TP ratio subsets, the low TN:TP ratio streams were dominantly located in the western half of the U.S. and the high TN:TP ratio streams were located in the eastern half (Table 1).

Results

Total variability

The median TN and TP concentrations were 0.39 and 0.01 mg l^{-1} respectively. The median TN:TP ratio was 55 and the probability of a TN:TP ratio $\leq$ 16:1 was 0.13 (497 of 3970 samples). The variability of TN:TP ratios was controlled more by TP than TN, which was demonstrated by a stronger correlation between TN:TP ratios and TP compared to TN (Fig. 2). A power relationship between the TN:TP ratios and TP concentrations showed an equation of $TN{:}TP = 3.09(TP)^{-0.70}$ with a coefficient of determination (R^2) of 0.59. The power relationship between the TN:TP ratios and TN concentrations showed an equation of $TN{:}TP = 63.1(TN)^{0.31}$ with an R^2 of 0.05. Similarly strong relationships between TP and TN:TP ratios have been demonstrated in lakes (Downing and McCauley 1992; Guildford and Hecky 2000).

Seasonal patterns

The NSNV curves showed the sinusoidal variation of Q in the entire data at the seasonal scale (Green and Finlay 2008). The precipitation subsets varied

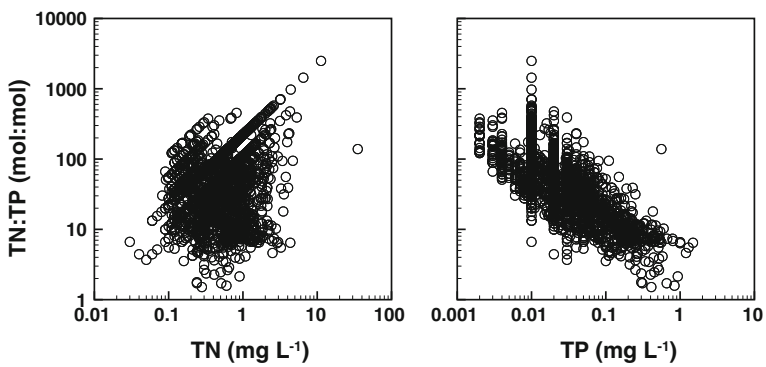

Fig. 2 Plots of TN:TP ratios as a function of TN concentration and TP concentration. Fitted power-law models show a stronger correlation for TP ($R^2 = 0.59$) than TN ($R^2 = 0.05$), suggesting that TN:TP variation is most related to TP variation

primarily through their peak seasonal Q, with humid climates peaking the earliest (day 52), semiarid climates peaking latest (day 155), and subhumid climates peaking between the humid and semiarid systems (day 113) (Green and Finlay 2008). This variation of time of peak seasonal Q was driven by the relative importance of snowmelt in each subset; more snowmelt equated to a later peak Q. The TN:TP ratio subsets showed clear differences, with Q* weight ratios in the low TN:TP set peaking earlier and with a higher magnitude than the high and intermediate TN:TP ratio sets (Fig. 3). Also, low seasonal flows were earlier and lower magnitude in the low TN:TP ratio sets than the high and intermediate TN:TP ratio sets. Overall, the low TN:TP ratio set showed more seasonal variation than the high and intermediate TN:TP ratio sets through the higher deviation from the median Q at peak and low flows. This was likely because the low TN:TP ratio set was composed mostly western, snowmelt-driven systems with strong seasonality.

For the entire dataset, TP* weight ratios were greatest during warmer months (i.e., between days 50 and 300), peaking at 4.0 on day 148. The lowest weight ratio of 1.5 occurred on day 355, which corresponds to winter baseflow conditions in many watersheds (Fig. 4a). A distinct secondary TP* weight ratio peak of 3.2 occurred later in the fall (day 288). The TP* weight ratio curves based on mean annual precipitation were most distinct during the first half of the year, and were more similar in late summer and fall. The semiarid TP* weight ratios

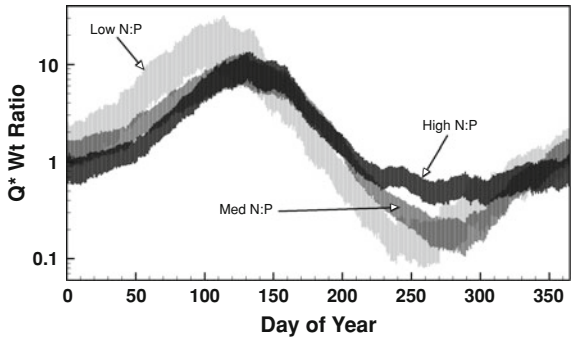

Fig. 3 Smoothed discharge values for subsets based on median TN:TP ratios. The high TN:TP ratio catchments are represented by the *darkest curve*, the low TN:TP ratios by the *lightest curve*, and the intermediate ratios by the intermediately *dark curve*. Curves for discharge for the entire data set and the climate subsets are presented in Green and Finlay (2008)

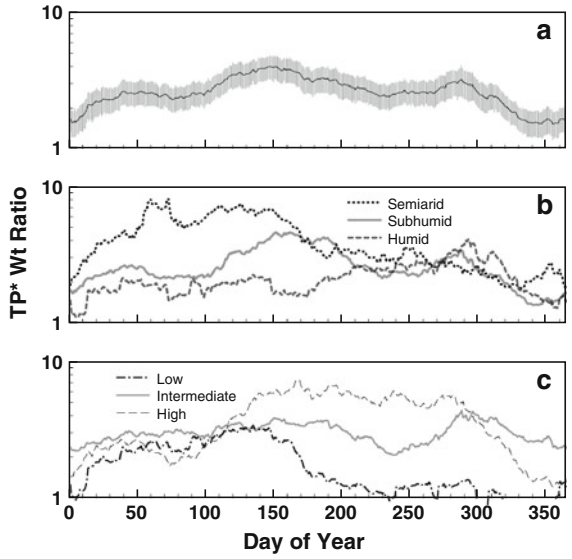

Fig. 4 Smoothed curves of TP from **a** all watersheds, **b** subsets based on mean annual precipitation, and **c** median TN:TP ratio. The *vertical lines* in frame **a** show the 95% confidence interval

showed the earliest and greatest magnitude peak (8.1 at day 72), the subhumid curve peaked twice (4.6 at day 152 and 3.4 at day 288), and the humid watershed showed one peak in the fall (4.1 at day 293; Fig. 4b). All three subsets based on median TN:TP ratio showed similar TP* seasonal dynamics during winter and early spring (i.e. prior to day 110), followed by distinctly different seasonal dynamics thereafter (Fig. 4c). High TN:TP ratio watersheds showed high TP* weight ratios between days 110 and 300. Intermediate TN:TP ratio watersheds showed a relatively constant TP* weight ratio throughout the year, except for a small peak at day 288. The TP* weight ratios in the low TN:TP ratio watersheds decreased after day 120 and remained low for the remainder of the year (Fig. 4c).

The TN dynamics of the TN:TP ratio subsets were largely similar indicating a seasonal dynamic with highest TN* weight ratios in the winter and spring followed by lower weight ratios in the late-summer and autumn (Fig. 5). The seasonal patterns are similar to the global TN curve and subsets of the global data based on drainage area and mean annual precipitation (Green and Finlay 2008). The main difference between the curves was that low TN:TP ratio streams had higher spring TN* weight ratios than the other subsets.

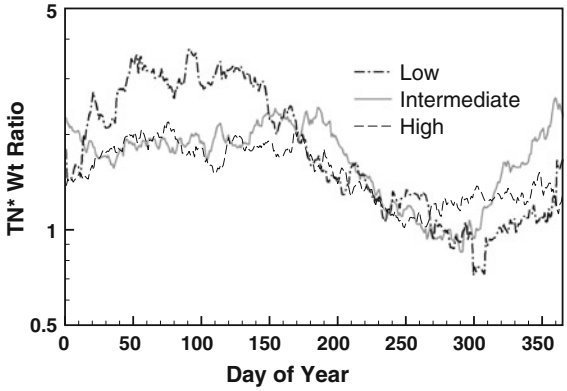

Fig. 5 Smoothed curves of TN data subsets based on median TN:TP ratio. Note that Green and Finlay (2008) presents the global and climate subset TN curves

The TN:TP* weight ratio curve based on all data appeared as an inversion of the TP curve, reaching a minimum of 0.63 on day 289, a secondary trough of 0.66 on day 155, and a maximum of 1.43 on day 359 (Fig. 6a). Subsets of the data based on mean annual precipitation and median TN:TP ratio had similar seasonal trends, with subtle differences appearing at specific times of the year. The main difference in mean annual precipitation classes was around day 300 when TN:TP* weight ratios were highest in the semiarid subset and lowest in the humid subset

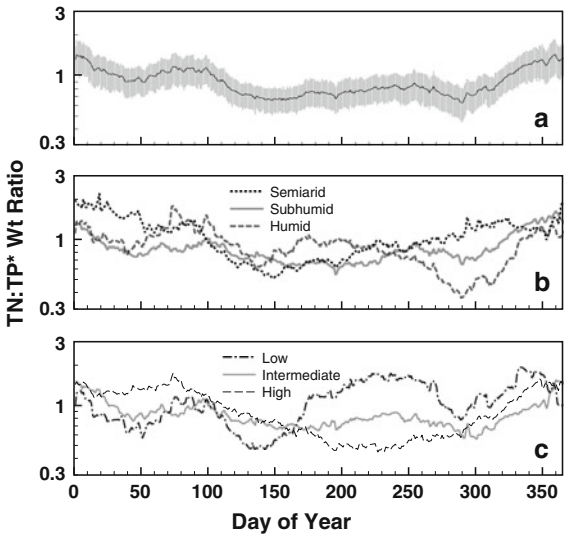

Fig. 6 Smoothed curves of TN:TP form **a** all watersheds, **b** subsets based on mean annual precipitation, and **c** median TN:TP ratio. The *vertical lines* in frame **a** show the 95% confidence interval

(Fig. 6b). The most visible difference amongst the median TN:TP ratio subsets was around day 230 when low TN:TP ratio streams had the highest TN:TP* weight ratios and high TN:TP ratio streams had the lowest TN:TP* weight ratios (Fig. 6c). Also, the low TN:TP ratio streams showed much more variable weight ratios with four distinct high-points at days 5, 87, 225, and 332.

Seasonal relationship between TN:TP ratios and discharge

The Q^* and TN:TP* weight ratio curves were plotted against one another to demonstrate the hydrologic influence on seasonal trends of TN:TP ratios. The global curve shows a clockwise loop (Fig. 7a), indicating hysteresis of the seasonal dynamics (Evans and Davies 1998). Winter produces a hydrologically mediated spike of TN:TP* weight ratios, followed by a secondary peak in spring as the Q^* weight ratio reaches its maximum. As the Q^* weight ratios decrease, the TN:TP* weight ratio changes very little.

Watershed subsets based on mean annual precipitation showed distinct differences. The humid watershed hysteresis loop shows a generally positive relationship between TN:TP* weight ratios and Q^* weight ratios with complex hysteresis (Fig. 7b). During the rising limb of the annual hydrograph, the TN:TP* weight ratios increase rapidly, but decline prior to reaching the maximum Q^* weight ratio. The falling limb of the annual hydrograph shows an opposite dynamic of rapidly decreasing TN:TP* weight ratios followed by a slight increase prior to minimum Q^* weight ratios. The subhumid watershed curve appears much more similar to the global curve than the humid and semiarid watershed curve (Fig. 7c). The semiarid watershed subset shows a negative relationship that was almost opposite to that of the humid watershed curve. The less complex form of the relationship suggests much simpler TN:TP ratio dynamics compared to the humid watersheds (Fig. 7d). The lack of a clear hysteresis curve indicates a system with two water source end-members (Evans and Davies 1998): a low N:P ratio source that contributes with increasing Q and a higher N:P ratio source that appears at lower flows.

A similar analysis based on the median TN:TP ratio subsets shows that high and low TN:TP ratio watersheds have fundamentally different responses to

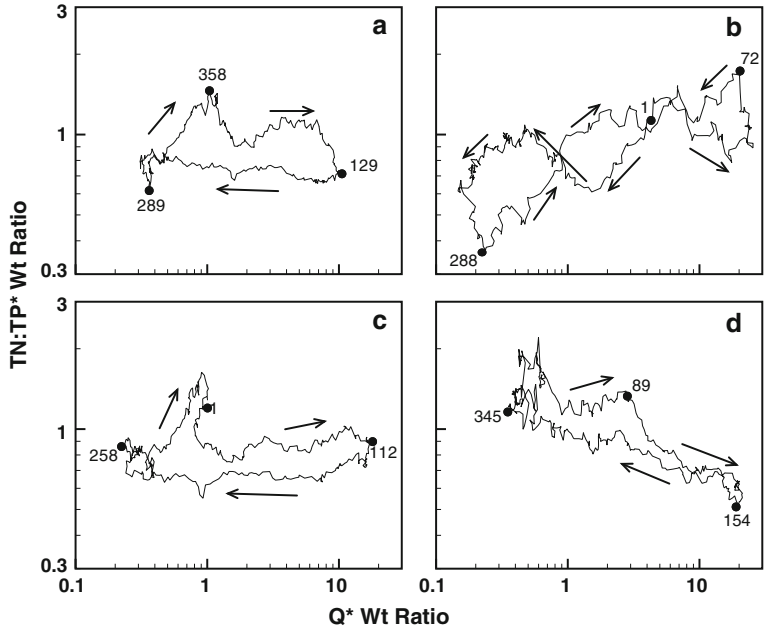

Fig. 7 Plots of TN:TP* weight ratio curves from Fig. 4a and b versus Q^* weight ratio curves from Green and Finlay (2008). The plots show **a** all data, **b** humid, **c** subhumid, and **d** semiarid watershed subsets. *Points* indicate the day of year on the curve and *arrows* indicate the seasonal progression of each curve

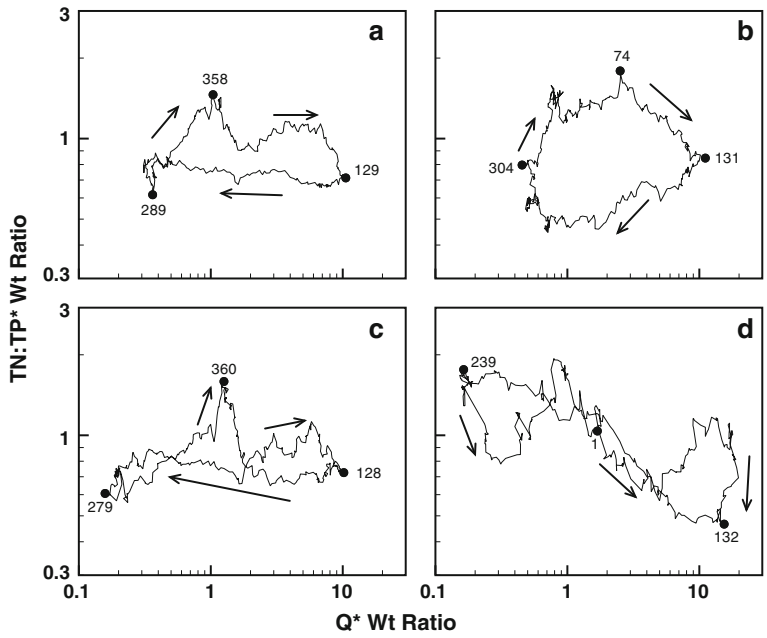

Fig. 8 Plots of TN:TP* weight ratio versus Q^* weight ratio in median TN:TP ratio watershed classes. The plots show **a** all data, **b** high median TN:TP ratio, **c** intermediate median TN:TP ratio, and **d** low median TN:TP ratio watershed subsets. *Points* indicate the day of year on the curve and *arrows* indicate the seasonal progression of each curve

changing discharge and seasonality (Fig. 8). The high TN:TP ratio watersheds indicate clear cyclical hysteresis with clockwise progression through the TN:TP* weight ratio versus Q^* weight ratio relationship (Fig. 8b). Such circular hysteresis indicates a continuously changing TN:TP ratio in source waters or continuously changing source waters with different TN:TP ratios throughout the year. While hysteresis is clear in the relationship from the high TN:TP ratio watershed subset, the low TN:TP ratio subset shows a drastically different relationship. The low TN:TP ratio curve shows two general characteristics (Fig. 8d). First, hysteresis looping is apparent at the lowest and highest Q^* weight ratios; counterclockwise at lowest Q^* weight ratios and clockwise at highest Q^* weight ratios. However, the two hysteresis

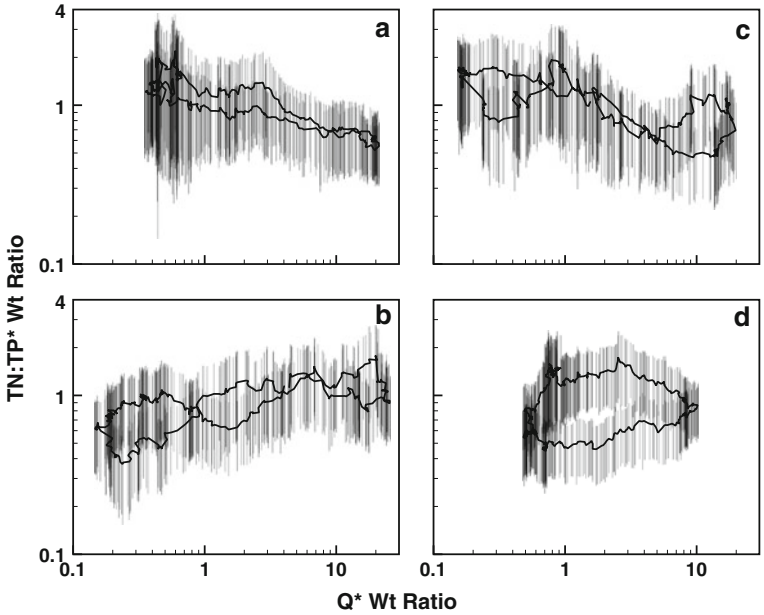

Fig. 9 Plots of TN:TP* weight ratio versus Q^* weight ratio relationships with vertical lines indicating the 95% confidence intervals around the TN:TP* weight ratios from the **a** semiarid, **b** humid, **c** low median TN:TP ratio, and **d** high median TN:TP ratio data subsets

loops are connected by a negative relationship that displays no hysteresis. This relationship indicates changing chemistry of source waters at low and high discharge, but a simple two-source model at times in between. As observed for the precipitation subsets, the intermediate TN:TP ratio subset appears very similar to the global relationship (Fig. 8a, c).

Visualization of the difference between the end member hysteresis curves (arid versus humid and low TN:TP versus high TN:TP) was aided by including the 95% confidence intervals around the TN:TP* weight ratios (Fig. 9). The confidence intervals for the Q^* weight ratios were substantially smaller than the TN:TP* weight ratios, and thus were not shown. The 95% confidence intervals overlap on the arid, humid, and low TN:TP ratio subsets, suggesting that the apparent hysteresis in the curves is not distinct. However, the hysteresis in the high TN:TP ratio subset was clearly different from that of intermediate and low TN:TP subsets as evidenced by non-overlapping confidence intervals.

Isolating the relationship between TN:TP ratios and discharge

Scatter plot thinning displayed the relationship between stream water TP concentrations and Q. The TP* $Quad_{II:III}$ ratio, which approximates the likelihood of a data point being greater than the median concentration and below the reference Q percentile, decreased with P_Q, with the greatest uncertainty occurring at low discharge percentiles (Fig. 10a). The TP* $Quad_{I:IV}$ ratio, which approximates the likelihood of a data point being greater than the median concentration and greater than the reference Q percentile, increased exponentially with increasing P_Q (Fig. 10b). This trend shows a linear increase in the $Quad_{I:IV}$ ratio between the 1st and 70th percentile followed by a deviation from the linear trend, possibly representing a threshold for hydrologic mobilization and transport of particulate P.

Data subsets of the global TP* $Quad_{II:III}$ ratio curve displayed similar patterns with one exception for both the climate and TN:TP ratio subsets. For the climate subsets, streams in humid climates showed a greater likelihood of super-median TP concentrations at low flows than the subhumid and semiarid climates (Fig. 10c). For the median TN:TP ratio subsets, streams with low TN:TP ratios appeared to have the greatest likelihood of sub-median TP concentrations at low flow. Streams across all climates and median TN:TP ratios appeared to transport TP in a similar pattern at high flows (Fig. 10d, f).

Trends of the TN* $Quad_{II:III}$ and $Quad_{I:IV}$ ratio from the different median TN:TP ratio groups show similar patterns as those from Green and Finlay (2008), with an apparent depression of TN

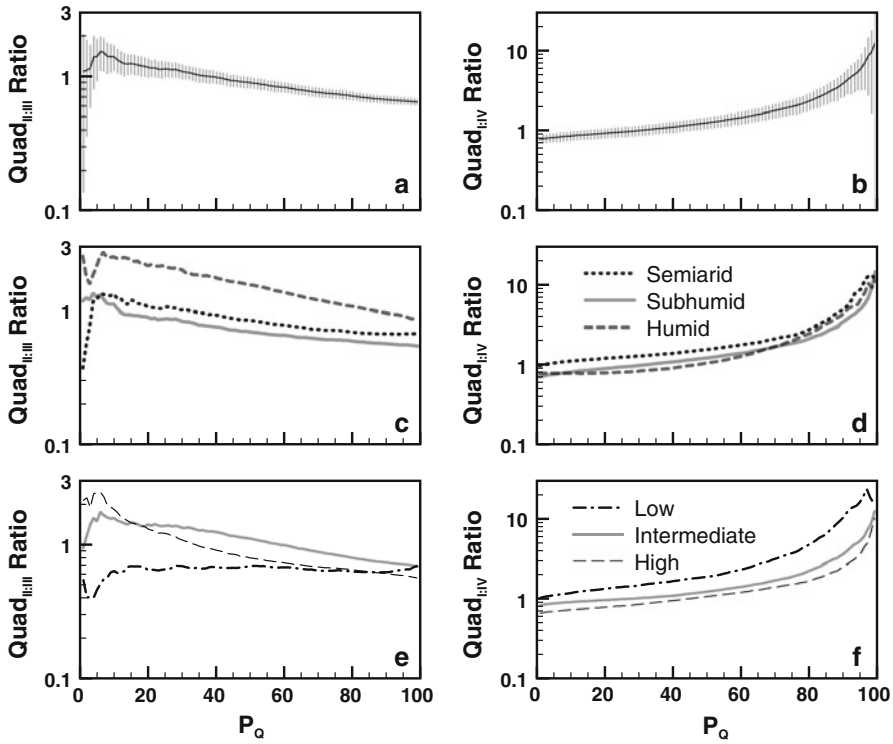

Fig. 10 Curves of total phosphorus **a** $Quad_{II:III}$ and **b** $Quad_{I:IV}$ ratios as a function of discharge percentile (P_Q) using the global data. Curves from data subsets based on mean annual precipitation (**c** and **d**) and median observed TN:TP ratio (**e** and **f**) are also shown

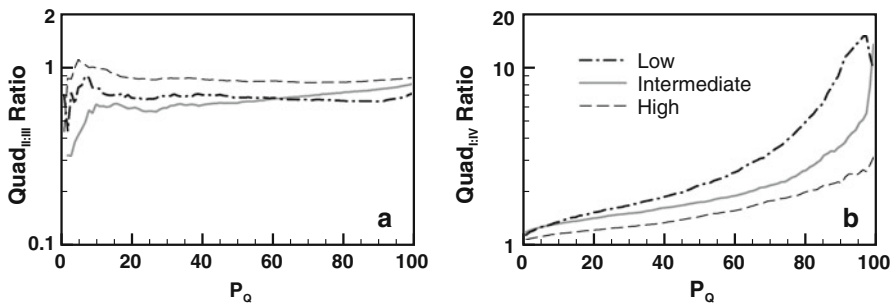

Fig. 11 Curves of total nitrogen **a** $Quad_{II:III}$ and **b** $Quad_{I:IV}$ ratios as a function of P_Q using data subsets based on median observed TN:TP ratio

concentrations at lowest Q rates (Fig. 11a) and increasing TN mobilization at with increasing Q (Fig. 11b).

The global TN:TP data showed that the TN:TP* $Quad_{II:III}$ ratio increased approximately linearly with P_Q from about 0.6 to 1.05 (Fig. 12a). The $Quad_{I:IV}$ ratios from the global data decreased exponentially with increasing P_Q from 0.95 to 0.2 (Fig. 12b). Separating the data into subsets based on mean annual precipitation showed some differences across climate types. The $Quad_{II:III}$ ratio curves from the precipitation subsets indicated distinct differences between the three groups (Fig. 12c). Humid climate $Quad_{II:III}$ ratios increased linearly with P_Q, similar, with a greater slope than the subhumid climate subset. The semiarid climate subset showed a drastic decrease from 4.4 at P_1 to 0.95 at P_{10}, followed by relative stability near a ratio of 1. These curves accentuate the different TN:TP dynamics occurring at low flows in different climates, which is discussed further below. All three climate classes showed remarkable similarity between their $Quad_{I:IV}$ ratio curves (Fig. 12d) and the global curve (Fig. 12b), suggesting similar transport and biogeochemical trends with increasing Q. The classification of data subsets by median TN:TP ratios differentiated low TN:TP ratio streams from other streams. While the TN:TP* $Quad_{II:III}$ ratio was depressed at low Q rates

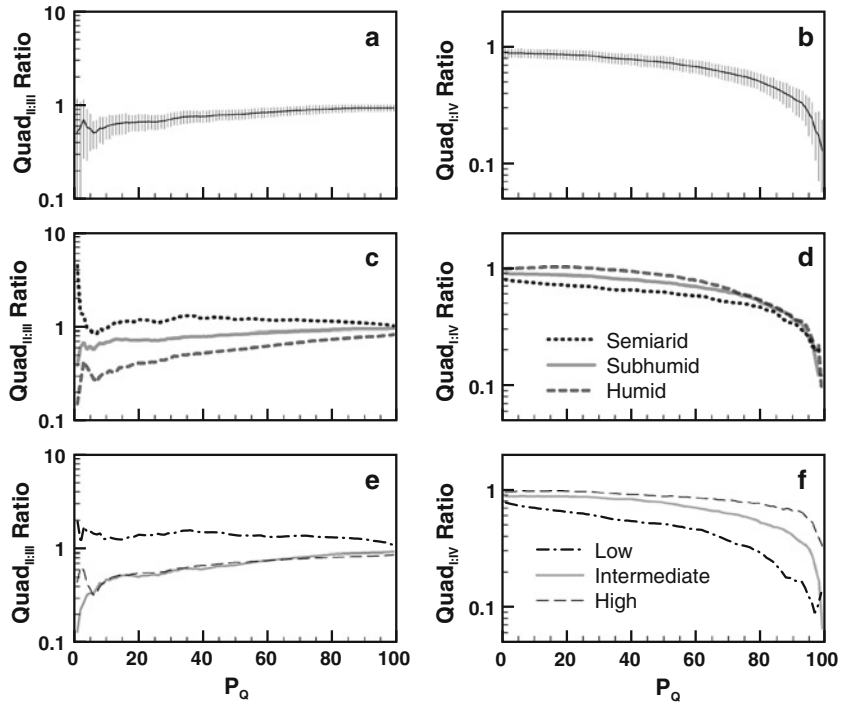

Fig. 12 Curves of TN:TP ratio **a** $Quad_{II:III}$ and **b** $Quad_{I:IV}$ ratios as a function of P_Q using the global data. Curves from data subsets based on mean annual precipitation (**c** and **d**) and median observed TN:TP ratio (**e** and **f**) are also shown

in high and intermediate median TN:TP ratio streams, low median TN:TP ratio streams remained relatively constant at a ratio just above 1 (Fig. 12e). The TN:TP* $Quad_{I:IV}$ ratio curves demonstrated that TN:TP ratios tend to decrease with increasing Q more readily in low TN:TP ratio streams compared to high and intermediate TN:TP ratio streams (Fig. 12f).

Discussion

Conceptually, we view control of the TN, TP, and TN:TP patterns as arising from dynamics of source material availability (i.e., terrestrial sources), material transport (i.e., hydrologic flow paths and the connectivity of those paths), and biogeochemical reactions during transport. The NSNV and NTNV methods are exploratory and synthesis techniques, thus material availability, transport, or biogeochemical reaction mechanisms driving the resulting patterns cannot be strictly isolated. However, our application of the methods attempts to isolate the hydrologic control of TN, TP, and TN:TP ratios. Here we place the NSNV and NTNV patterns in the context of previous studies to help deduce likely mechanisms driving the patterns.

Hydrologic connections across the landscape and TN:TP ratios

The seasonal-scale results demonstrate characteristic trends in the 57-watershed data set, allowing a generalization of seasonal patterns in watersheds lightly modified by human activities. The picture of seasonal TP dynamics (Fig. 4a) generally agreed with previous studies from individual watersheds (Mulholland and Hill 1997; Bowes et al. 2005; Jarvie et al. 2008), with higher P concentrations arising spring through fall due to enhanced hydrologic transport. Similarly, the seasonal patterns of TN:TP ratios from this synthesis (Fig. 6a) showed peak N:P ratios occurring in the winter, similar to previous site-specific studies (Meyer et al. 1981; Wold and Hershey 1999). Synthesis of the general temporal variability of TP and TN:TP ratios provides an average condition to which other watersheds can be compared. In both cases, disaggregating the TP and TN:TP trends shows different seasonal trends arising from mean annual precipitation and median TN:TP ratio. While the seasonal trends of TP and TN:TP ratios provided by the NSNV technique show differences between the data subsets, more distinct differences across systems

appeared when the TN:TP* weight ratio was plotted against the Q^* weight ratio.

The hysteresis curves from the seasonal Q^* and TN:TP* weight ratio curves in Fig. 7 resulted from distinctly different watershed dynamics between the precipitation classes. Specifically, we hypothesize that the different TN:TP* versus Q^* weight ratio relationships and associated hysteresis looping across data subsets results from different coupled hydrologic connectivity (Western et al. 2001; Stieglitz et al. 2003; Jencso et al. 2009) and nutrient demand by the watershed.

For example, in the humid watersheds, soil water is more available for transport during the late fall and winter because of plant dormancy and a lack of freezing temperatures (i.e., water immobilization). This same period is a time of least biological demand in the terrestrial ecosystem, thus N and P are more available during the period of greatest hydrologic transport. Persistent water transport to the stream will be via soil water, which is more conducive to N transport because of the sorptive nature of P (Green et al. 2007). Phosphorus transport from watersheds is generally much more episodic, strongly increasing during overland flow events, which are more stochastic in nature (thus less reflected in the NSNV curves). Thus, as Q increases during a season, N concentration increases, but P concentration remains similar (as shown in Fig. 4c).

In the humid watersheds, the complicated hysteretic looping also indicates a changing mix of water from multiple water sources (>2 sources) contributing to Q throughout the year. Such looping would require a persistent but evolving hydrologic connection between water in the landscape and the stream—and soil moisture likely plays an important role in that connectivity. For example, during the dormant season, N would be transported through the subsurface (soils or ground water) to the stream, flushing any accumulation of N during the part of the year when terrestrial demand keeps soil moisture (and thus hydrologic connectivity) lower (e.g., Creed et al. 1996; Hill et al. 1999; Kaushal et al. 2008).

Semiarid watersheds, on the other hand, have less consistent soil moisture throughout the year compared to more humid watersheds (Famiglietti et al. 2008), thus they likely have a less persistent connection between the landscape and streams. The less persistent connectivity decouples seasonal variation of terrestrial biogeochemistry from stream nutrient chemical composition. The main terrestrial signal in the seasonal TN:TP variability is snowmelt which apparently releases water with a low TN:TP ratio. This appears as a narrow looping relationship in the semiarid watersheds (Fig. 7d) where hydrologic connectivity is seasonally ephemeral: high TN:TP ratio waters at low Q and low TN:TP ratio waters at high Q when the system is most hydrologically connected. The decreasing TN:TP* weight ratios with increasing Q^* was apparently being driven by very high early season TP concentrations because both TN and TP increase during the spring, yet the TN:TP ratio declined (Figs. 7b, 4b and Fig. 7a in Green and Finlay 2008). We hypothesize that the enrichment of the stream waters with TP during spring runoff is likely due to snow melt driven transport of P. Phosphorus mobilization can be greatly elevated following the winter relative to other times of the year due to freeze-thaw cycles which enhance microbial and fine root P release (Fitzhugh et al. 2001), and increased particulate P losses can occur due to overland flow during snowmelt.

Differences in watershed hydrologic connectivity across climates have been demonstrated (Stieglitz et al. 2003; Newman et al. 2006), with important implications for stream water N:P ratios (Green and Wang 2008; Frost et al. 2009). An N or P source on the landscape can only influence stream water concentrations and N:P ratios if it is hydrologically connected to the stream. Shallow and deep subsurface pathways in humid watersheds can facilitate a persistent connection between nutrient sources and the stream. A stable connectivity allows the variation of terrestrial dynamics to become apparent in stream water concentrations. Alternatively, more variable connections between landscape units, like in arid climates, make terrestrial dynamics difficult to detect in stream water. Thus, in semiarid watersheds we suggest that the variability of N:P ratios are more strongly linked to variability of connectivity as opposed to variability of terrestrial biogeochemistry.

While previous work on humid and semiarid watersheds aided our interpretation of precipitation subsets, no work has compared the hydrology of low and high TN:TP ratio watersheds. The fact that the Q^* weight ratio curves between the median TN:TP ratio subsets were different, especially at high and low flows, provides evidence that hydrology plays an

important role in the spatial variation of stream water TN:TP ratios. The different seasonality of TN:TP ratio subsets was also most evident at low flows, when periphyton are most likely to accrue biomass. Thus, we expect that in-stream dynamics are causing the differences between the TN:TP* weight ratio subsets at low flows. However, mechanisms leading to the different hysteresis curves in Fig. 8 are less clear. The circular variation of the high TN:TP ratio subset hysteresis curve (Fig. 8b) shows seasonal evolution of N and P sources that has a shifted phase compared to Q; similar trends, only with different timing of the peak weight ratio. This evolution may arise because of the changing hydrologic connectivity throughout the seasons or the changing TN:TP ratios of the source waters or both. The low TN:TP ratio subset shows more complex dynamics, but the statistical certainty of those complexities are questionable (Fig. 9c).

TN:TP ratios at high and low flows

The results from the NTNV analysis identified a general pattern of event-scale variability of TN:TP ratios previously observed in some studies of individual watersheds, while providing further insight into factors that mediate event responses. The $Quad_{I:IV}$ ratio curves showed a general decrease of TN:TP* with Q* (Fig. 12b, d, f), suggesting that TN:TP ratios consistently decline across all watershed types during high flows. Similar trends have been observed in time-series of N:P ratios during storm events (Correll et al. 1999; Green et al. 2007). Of the different data subsets, the low median TN:TP ratio set showed the most distinct behavior, with a more linear decrease of $Quad_{I:IV}$ ratios with increasing Q. Thus, increases of Q from relatively low flows immediately lower TN:TP ratios in low TN:TP ratio streams, while the other types respond strongly only at very high flows. The results from the $Quad_{II:III}$ ratio curves demonstrated elevated TN:TP* within the lowest 10th percentile Q only in semiarid and low TN:TP ratio streams (Fig. 12c). This suggests fundamentally different controls on TN:TP ratios in these two watershed classes, compared to the others. Possible controls include high ground water N concentrations (compared to other water sources) in low TN:TP ratio and semiarid watersheds (e.g., Walvoord et al. 2003) or low denitrification rates at low flows compared to other watershed subsets. Also, it should be noted that the low TN:TP ratio and semiarid streams were more likely to be below the Redfield ratio of N:P = 16:1. Thus, the potential for N limitation of primary production in these streams, as opposed to P limitation in the other classes, would alter biological dynamics in the stream and produce a different demand for N and P.

The TN:TP ratio subsets showed the importance of temporal variations of Q on average TN:TP ratios. Green et al. (2007) suggested that pulses of low N:P ratio water during storm events may be damped to produce persistent low stream water N:P ratios at larger scales. The increased sensitivity of low TN:TP ratio streams to Q relative to other streams suggests that temporal pulses of low TN:TP ratio water may be important to maintaining low median TN:TP ratios locally, not only downstream (Fig. 11f). Low TN:TP ratios are generated at much lower Q percentiles in the low TN:TP ratio watersheds, which appears to have an important influence on maintaining low median TN:TP ratios. Possible mechanisms for converting low TN:TP pulses to low median TN:TP ratios are in-stream biological, chemical and physical retention of TP and hydraulic dispersion during longitudinal transport (more details are discussed in Green et al. (2007)). Also, the $Quad_{II:III}$ ratio curves show that as Q decreases in low TN:TP ratio watersheds, TN:TP ratios slightly increase and remain above median ratios (Fig. 12e). The other TN:TP ratio classes which show depressed TN:TP ratios at lower Q percentiles may be explained by increased water residence time in side pools or the hyporheic zone which are known to enhance denitrification (e.g., Hill et al. 1998).

Implications

We highlight the importance of hydrologic processes to stream water TN:TP ratios by analyzing temporal and hydrologic dynamics at a much larger scale than previous efforts. Our analyses establish the generality of previous work in individual watershed that has identified hydrologic pathways as a control on N:P ratios in lotic ecosystems (Watson et al. 1981; Correll et al. 1999; Saunders et al. 2006; Green et al. 2007; Green and Wang 2008). Most significantly, we bring the concept of hydrologic connectivity to the forefront as a fundamental mechanism

that warrants further investigation (e.g., Frost et al. 2009). Many previous authors who have addressed controls on TN:TP ratios have focused on sources of N and P, but have neglected the role of hydrologic connections across the landscape. This analysis suggests that increased attention to hydrology will produce much more mechanistic understanding of the variability of N:P ratios in streams and their receiving waters.

Furthermore, the importance of hydrology and connectivity highlights the physical nature of drivers in lotic ecosystems. Decomposition of organic matter—the driver of marine water N:P ratios—is unlikely as a primary control on stream water N:P ratios, explaining why Redfield ratios (N:P = 16:1) in stream water are much less likely than in lakes and marine systems (Meybeck 1982; Downing and McCauley 1992; Hecky et al. 1993; Guildford and Hecky 2000; Giani et al. 2003; Turner et al. 2003; Babiker et al. 2004). Even at low flows, in-stream controls on nutrient concentrations are complicated by downstream transport (Brookshire et al. 2009).

The importance of incorporating hydrodynamics into the understanding of stream ecosystems has been recognized in the past through the combination of ecological stoichiometry and nutrient spiraling concepts (Newbold et al. 1982). Taking these ideas one step further by including concepts of stream flow generation is fundamental to understanding stream ecosystems and their elemental foundations. Thus, catchment hydrology must be incorporated into a broader understanding of stream ecology that integrates terrestrial biogeochemistry, hydrologic connections across the landscape, and the resulting impact on aquatic biogeochemistry.

Acknowledgments We thank two anonymous reviewers whose insights improved the communication of this work. This work was supported by the STC program of the National Science Foundation via the National Center for Earth-Surface Dynamics under Agreement EAR-0120914. Also, M.G. was supported via a USDA National Needs Fellowship.

References

Arbuckle KE, Downing JA (2001) The influence of watershed land use on lake N:P in a predominantly agricultural landscape. Limnol Oceanogr 46:970–975

Babiker IS, Mohamed MAA, Komaki K, Ohta K, and Kato K (2004) Temporal variations in the dissolved nutrient stocks in the surface water of the western North Atlantic Ocean. J Oceanogr 60:553–562

Billen G et al (1991) N, P, and Si retention along the aquatic continuum from land to ocean. In: Mantoura RFC, Martin J-M, Wollast R (eds) Ocean margin and processes in global change. Wiley, New York

Borchardt MA (1996) Nutrients. In: Stevenson RJ, Bothwell ML, Lowe RL (eds) Algal ecology. Academic Press, San Diego

Bowes MJ, Leach DV, House WA (2005) Seasonal nutrient dynamics in a chalk stream: the River Frome, Dorset, UK. Sci Total Environ 336:225–241

Brookshire ENJ, Valett HM, Gerber S (2009) Maintenance of terrestrial nutrient loss signatures during in-stream transport. Ecology 90:293–299

Correll DL, Jordan TE, Weller DE (1999) Transport of nitrogen and phosphorus from Rhode River watersheds during storm events. Water Resour Res 35:2513–2521

Creed IF, Band LE, Foster NW, Morrison IK, Nicolson JA, Semkin RS, Jeffries DS (1996) Regulation of nitrate-N release from temperate forests: a test of the N flushing hypothesis. Water Resour Res 32(11):3337–3354

Detenbeck NE, Elonen CM, Taylor DL, Anderson LE, Jicha TM, Batterman SL (2004) Region, landscape, and scale effects in Lake Superior tributary water quality. J Am Water Resour As 40:705–720

Dodds WK (2003) Misuse of inorganic N and soluble reactive P concentrations to indicate nutrient status of surface waters. J North Am Benthol Soc 22:171–181

Downing JA and McCauley E (1992) The nitrogen–phosphorus relationship in lakes. Limnol Oceanogr 37:936–945

Evans C, Davies TD (1998) Causes of concentration/dicharge hysteresis and its potential as a tool for analysis of episode hydrochemistry. Water Resour Res 34:129–137

Famiglietti JS, Ryu D, Berg AA, Rodell M, Jackson TJ (2008) Field observations of soil moisture variability across scales. Water Resour Res 44:W01423. doi:10.1029/2006WR005804

Fitzhugh RD, Driscoll CT, Groffman PM, Tierney GL, Fahey TJ, Hardy JP (2001) Effects of soil freezing disturbance on soil solution nitrogen, phosphorus, and carbon chemistry in a northern hardwood ecosystem. Biogeochemistry 56:215–238

Francoeur SN, Biggs BJF, Smith RA, Lowe RL (1999) Nutrient limitation of algal biomass accrual in streams: seasonal patterns and a comparison of methods. J North Am Benthol Soc 18:242–260

Frost PC, Kinsman LE, Johnston CA, Larson JH (2009) Watershed discharge modulates relationships between landscape components and nutrient ratios in stream seston. Ecology 90:1631–1640

Giani M, Savelli F, Boldrin A (2003) Temporal variability of particulate organic carbon, nitrogen and phosphorus in the Northern Adriatic Sea. Hydrobiologia 494:319–325

Green MB, Finlay JC (2008) Detecting characteristic hydrological and biogeochemical signals through nonparametric scatter plot analysis of normalized data. Water Resour Res 44:W08455. doi:10.1029/2007WR006509

Green MB, Fritsen CH (2006) Spatial variation of nutrient balance in the Truckee River, California-Nevada. J Am Water Resour Assoc 42:659–674

Green MB, Wang D (2008) Watershed flow paths and stream water nitrogen-to-phosphorus ratios under simulated precipitation regimes. Water Resour Res 4:W12414. doi:10.1029/2007WR006139

Green MB, Nieber JL, Johnson G, Magner J, Schaefer B (2007) Flow path influence on an N:P ratio in two headwater streams: a paired watershed study. J Geophys Res 112:G03015. doi:10.1029/2007JG000403

Green MB, Wollheim WM, Basu N, Gettel G, Rao PS, Morse N, Stewart R (2009) Effective denitrification scales predictably with water residence time across diverse systems. Available from Nature Precedings: http://hdl.handle.net/10101/npre.2009.3520.1

Grimm NB, Fisher SG, Mickley WL (1981) Nitrogen and phosphorus dynamics in hot desert streams of Southwestern USA. Hydrobiologia 83:303–312

Guildford SJ, Hecky RE (2000) Total nitrogen, total phosphorus, and nutrient limitation in lakes and oceans: is there a common relationship?. Limnol Oceanogr 45:1213–1223

Hecky RE, Campbell P, Hendzel LL (1993) The stoichiometry of carbon, nitrogen, and phosphorus in particulate matter of lakes and oceans. Limnol Oceanogr 38:709–724

Hill AR, Labadia CF, Sanmugadas K (1998) Hyporheic zone hydrology and nitrogen dynamics in relation to the streamed topography of a N-rich stream. Biogeochemistry 42:285–310

Hill AR, Kemp WA, Buttle JM, Goodyear D (1999) Nitrogen chemistry of subsurface storm runoff on forested Canadian Shield hillslopes. Water Resour Res 35:811–821

Horne AJ, Goldman CR (1994) Limnology. McGraw Hill, New York

House WA, Warwick MS (1998) Hysteresis of the solute concentration. Water Res 32:2279–2290

Jarvie HP, Withers PJA, Hodgkinson R, Bates A, Neal M, Wickham HD, Harman SA, Armstrong L (2008) Influence of rural land use on streamwater nutrients and their ecological significance. J Hydrol 350:166–186

Jencso KG, McGlynn BL, Gooseff MN, Wondzell SM, Bencala KE, Marshall LA (2009) Hydrologic connectivity between landscapes and streams: transferring reach- and plot-scale understanding to the catchment scale. Water Resour Res 45:W04428. doi:10.1029/2008WR007225

Kaushal SS, Groffman PM, Band LE, Shields CA, Morgan RP, Palmer MA, Belt KT, Swan CM, Findlay SEG, Fisher GT (2008) Interaction between urbanization and climate variability amplifies watershed nitrate export in Maryland. Environ Sci Technol 42:5872–5878. doi:10.1021/es800264f

McGroddy ME, Baisden WT, Hedin LO (2008) Stoichiometry of hydrological C, N, and P losses across climate and geology: an environmental matrix approach across New Zealand primary forests. Global Biogeochem Cycles 22:GB1026. doi:10.1029/2007GB003005

Meybeck M (1982) Carbon, nitrogen, and phosphorus transport by world rivers. Am J Sci 282:401–450

Meyer JL, Likens GE, Sloane J (1981) Phosphorus, nitrogen, and organic carbon flux in a headwater stream. Arch Hydrobiol 91:28–44

Mulholland PJ, Hill WR (1997) Seasonal patterns in streamwater nutrient and dissolved organic carbon concentrations: separating catchment flow path and in-stream effects. Water Resour Res 33:1297–1306

Newbold JD, ONeill RV, Elwood JW, VanWinkle W (1982) Nutrient spiralling in streams. Implications for nutrient limitation and invertebrate activity. Am Nat 120(5): 628–652

Newman BD, Vivoni ER, Groffman AR (2006) Surface water-groundwater interactions in semiarid drainages of the American southwest. Hydrol Process 20:3371–3394. doi:10.1002/hyp.6336

Pacini N, Gachter R (1999) Speciation of riverine particulate phosphorus during rain events. Biogeochemistry 47: 87–109

Ptacnik R, Jenerette GD, Verschoor AM, Huberty AF, Solimini AG, Brookes JD (2005) Applications of ecological stoichiometry for sustainable acquisition of ecosystem services. Oikos 109:52–62

Redfield AC (1958) The biological control of chemical factors in the environment. Am Sci 46:205–221

Sabo JL, Post DM (2008) Quantifying periodic, stochastic and catastrophic variation in the environment using time series of environmental conditions. Ecol Monogr 78:19–40

Saunders TJ, McClain ME, Llerena CA (2006) The biogeochemistry of dissolved nitrogen, phosphorus, and organic carbon along terrestrial-aquatic flowpaths of a montane headwater catchment in the Peruvian Amazon. Hydrol Process 20:2549–2562. doi:10.1002/hyp.6215

Smith RA, Alexander RB, Schwarz GE (2003) Natural background concentrations of nutrients in streams and rivers of the conterminous United States. Environ Sci Technol 37:3039–3047

Stelzer RS, Lamberti GA (2001) Effects of N:P ratio and total nutrient concentration on stream periphyton community structure, biomass, and elemental composition. Limnol Oceanogr 46:356–367

Stieglitz M, Shaman J, McNamara J, Engel V, Shanley J, Kling GW (2003) An approach to understanding hydrologic connectivity on the hillslope and the implications for nutrient transport. Global Biogeochem Cycles 17:1105. doi:10.1029/2003GB002041

Turner RE, Rabalais NN, Justic D, Dortch Q (2003) Global patterns of dissolved N, P and Si in large rivers. Biogeochemistry 64:297–317. doi:10.1023/A:1024960007569

UNEP (2002) World's water cycle: schematic and residence time. In: UNEP/GRID-Arendal Maps and Graphics Library, Retrieved 16:19, October 2, 2008 from http://maps.grida.no/go/graphic/world_s_water_cycle_schematic_and_residence_time

Walvoord MA, Phillips FM, Stonestrom DA, Evans RD, Hartsough PC, Newman BD, Striegl RG (2003) A reservoir of nitrate beneath desert soils. Science 302:1021–1024. doi:10.1126/science.1086435

Watson VJ, Loucks OL, Wojner W (1981) The impact of urbanization on seasonal hydrologic and nutrient budgets of a small North American watershed. Hydrobiologia 77:87–96

Western AW, Blöschl G, Grayson RB (2001) Towards capturing hydrologically significant connectivity in spatial patterns. Water Resour Res 37:83–97

Wold AP, Hershey AE (1999) Spatial and temporal variability of nutrient limitation in 6 North Shore tributaries to Lake Superior. J North Am Benthol Soc 18:2–14